Optically induced spin wave dynamics in $[Co/Pd]_8$ antidot lattices with perpendicular magnetic anisotropy

S. Pal,[1] J. W. Klos,[2] K. Das,[1] O. Hellwig,[3] P. Gruszecki,[2] M. Krawczyk,[2,a)] and A. Barman[1,b)]
[1]*Thematic Unit of Excellence on Nanodevice Technology and Department of Condensed Matter Physics and Material Sciences, S. N. Bose National Centre for Basic Sciences, Block JD, Sector III, Salt Lake, Kolkata 700 098, India*
[2]*Faculty of Physics, A. Mickiewicz University in Poznan, Umultowska 85, 61-614 Poznań, Poland*
[3]*San Jose Research Center, HGST, a Western Digital Company, 3403 Yerba Buena Rd., San Jose, California 95135, USA*

We present an all-optical time-resolved measurement of spin wave (SW) dynamics in a series of antidot lattices based on $[Co(0.75\,nm)/Pd(0.9\,nm)]_8$ multilayer (ML) systems with perpendicular magnetic anisotropy. The spectra depend significantly on the areal density of the antidots. The observed SW modes are qualitatively reproduced by the plane wave method. The interesting results found in our measurements and calculations at small lattice constants can be attributed to the increase of areal density of the shells with modified magnetic properties probably due to distortion of the regular ML structure by the Ga ion bombardment and to increased coupling between localized modes. We propose and discuss the possible mechanisms for this coupling including exchange interaction, tunnelling, and dipolar interactions.

The perpendicular percolated media (PPM) have been proposed, as an alternative to the bit patterned media (BPM), towards achieving higher storage density in magnetic recording and as a potential candidate for magnonic devices.[1] The Co/Pd and Co/Pt continuous multilayers (MLs) with high perpendicular magnetic anisotropy (PMA) are already well studied for their possible applications in present day technology.[2,3] Pattering such MLs to nanoscale for fabricating PPM with interesting properties has recently triggered tremendous research. Study of magnetic properties on antidots based on Co/Pd MLs with varying Co layer thicknesses claims antiferromagnetic coupling to be responsible for the PMA in these structures.[4] For Co/Pt PMA antidot lattices (ADLs), the magnetic properties depend strongly on the antidot size and separation.[1,5] With increasing pore diameter, the domain-wall (DW) energy changes and the pinning field increases. Due to this increase in the DW pinning, the coercive field of the system also increases. However, the anisotropy near the rim of the pores, instead of being exactly perpendicular, gets a little bit tilted. With the increase in pore diameter, the perimeter increases, and, consequently, the tilting becomes more severe and degrades the PMA. It has also been studied[1,6] that the hindered DW movements due to holes control the magnetization reversal processes in these PMA ADLs.

On the other hand, for applications in magnonics,[7,8] the understanding of the magnetization dynamics is very important. So far, there have been a significant amount of studies on ultrafast magnetization dynamics and spin waves (SWs)[9–14] in ferromagnetic ADLs with in-plane anisotropy. However, a detailed study of the magnetization dynamics in ADLs with high PMA is still absent in the literature. Here, we present a systematic study of the dependence of the SW spectrum on the areal density of a series of ADLs based on $[Co(0.75\,nm)/Pd(0.9\,nm)]_8$ ML systems with PMA by using an all optical time-resolved magneto-optical Kerr effect (TR-MOKE) microscope. The observed SW modes are modelled by the plane wave method (PWM).

The $[Co(0.75\,nm)/Pd(0.9\,nm)]_8$ ML structures are deposited by dc magnetron sputtering using a confocal sputter up geometry.[2,15] The base pressure of the deposition chamber was 2×10^{-8} millibar, and the deposition was performed at 3 mTorr of Ar pressure. The ADLs are fabricated by focused ion beam (FIB) milling of the Co/Pd ML using liquid Ga^+ ions at 30 kV voltage and 20 pA beam current, which produce a spot size of about 8 nm. In our case, the antidot diameter (d) value is fixed at 100 nm and edge to edge separation (s) varies from 100 to 400 nm, and hence, the lattice constant $a = d + s$ varies from 200 to 500 nm. Each pattern covers an area of $8 \times 8\,\mu m^2$. Figure 1(a) presents the scanning electron micrographs of the ADLs. The measured a and d values are close to the nominal values. The ultrafast magnetization dynamics are measured by a custom-built TR-MOKE microscope in a two-colour optical pump-probe setup.[16] The second harmonic ($\lambda = 400$ nm, spot size $\sim 1\,\mu$m, fluence $= 18$ mJ cm^{-2}) of a Ti-sapphire oscillator was used to pump the dynamics, whereas the time delayed fundamental ($\lambda = 800$ nm, spot size ~ 800 nm, fluence $= 2.5$ mJ cm^{-2}) was used to probe the dynamics. The Kerr rotation was measured by an optical bridge detector as a function of the time-delay between the pump and probe beams. The external magnetic field (H) is tilted at a small angle ($\sim 10°$) to the surface normal of the sample.

Figure 1(b) presents typical TR-MOKE data obtained from the ADL with $a = 400$ nm at $\mu_0 H = 0.084$ T. The data shows characteristic ultrafast demagnetization (within 400–500 fs from the zero-delay) and fast and slow remagnetization signals. The precessional dynamics appears as an oscillatory signal on top of the decaying part of the TR-MOKE signal. A bi-exponential background is subtracted from the

a)krawczyk@amu.edu.pl
b)abarman@ybose.res.in

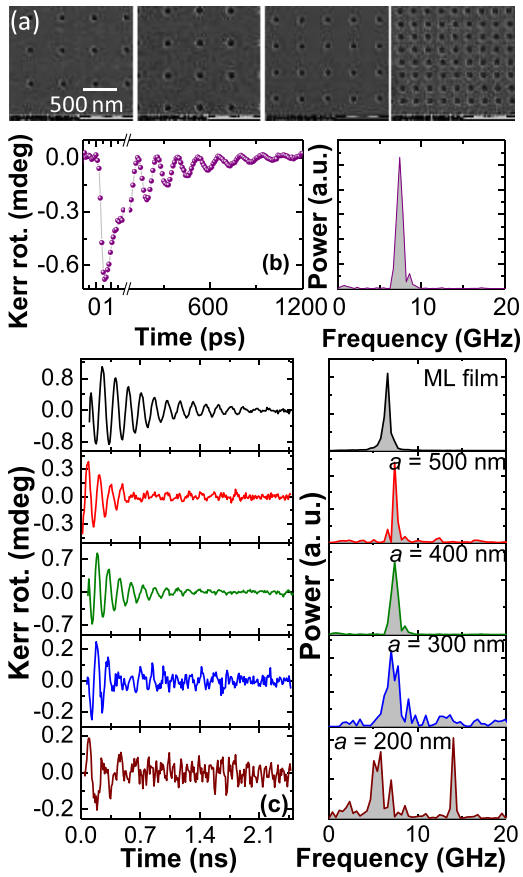

FIG. 1. (a) Scanning electron micrographs of the antidot lattices (ADLs) with lattice constant a varying as 500, 400, 300, and 200 nm. (b) Typical TR-MOKE signal and corresponding spin wave spectrum for ADL with $a = 400$ nm. (c) Areal density dependence of the TR-MOKE signal with the bi-exponential background subtracted and the spin wave spectra of the ADLs and a ML film at $\mu_0 H = 0.084$ T.

time-resolved data before performing the fast Fourier transform (FFT) to obtain the corresponding SW spectrum.

Figure 1(c) shows that the SW spectrum depends significantly on the areal density of the ADL. For $a = 500$ nm, an intense peak at frequency (f) of 7.4 GHz with small side lobes on both sides of the peak is found. The frequency of the intense peak is slightly greater than the frequency of the uniform mode of the continuous ML ($f = 6.64$ GHz). For $a = 400$ nm, this peak remains almost in the same position ($f = 7.42$ GHz) as for $a = 500$ nm. Interestingly, as a is reduced further, multiple SW modes start to appear. For $a = 300$ nm, there is a broad band of modes centred at around $f = 7.05$ GHz with a number of lower intensity modes in the higher frequency regime. A further drastic change is observed for the ADL with the smallest period, i.e., $a = 200$ nm. In this sample, there are two distinct bands, a broad band centred around $f = 5.64$ GHz and a narrow band centred around $f = 14.11$ GHz. The lower band experienced a significant red-shift as opposed to the other ADLs.

In Fig. 2(a), we plot the f vs. H result of the continuous ML. The data were fitted to the Kittel formula[2] to extract material parameters which will be used later in this article for theoretical calculations. As a uniform collective precession of the whole ML stack is observed for all field values, we assume the ML structure as an effective magnetic medium with parameters: saturation magnetization $M_S = 0.78 \times 10^6$ A/m,

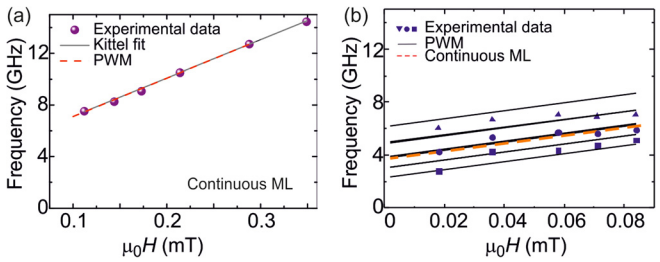

FIG. 2. (a) Dependence of frequency of spin wave mode on H for continuous Co/Pd ML. The TR-MOKE data (symbol), fit to the Kittel formula (solid line), and the PWM results (dashed line) using the same parameters are shown. (b) Dependence of frequencies of spin wave modes on H for ADLs with $a = 200$ nm (dots) along with the results from PWM calculations (solid lines) and continuous ML (dashed line).

gyromagnetic ratio $\gamma = 187$ GHz/T, and PMA field $\mu_0 H_{ani} = 1.119$ T. These values are in accordance with parameters found in previous measurements.[2] The bias field dependence of f in ADLs with $a = 200$ nm is presented in Fig. 2(b). Occurrence of multiple SWs at all H values is observed. The frequencies of the lower frequency modes decrease with decreasing H, whereas the highest frequency mode does not show any discernible dependence on H.

For interpretation of these intriguing experimental results, we have used PWM which is a suitable method for calculations of spectra of collective dynamics in periodic structures, also in thin films of ADL.[12,17–20] We have used material parameters (M_S, H_{ani}, and γ) obtained from Fig. 2(a), and, additionally, the effective exchange constant of the ML film, $A = 1.3 \times 10^{-11}$ J/m, was assumed.[21] The PWM results with this set of parameters match very well with the experimental data of continuous ML shown in Fig. 2(a). The calculated spectra of two low frequency SWs extending along the lateral dimensions of the ADLs and uniform across the ADL thickness as a function of a is shown in Fig. 3(a) with green dashed lines. We can see a monotonous increase of the frequencies of all SWs with decreasing a. From the calculated maps of amplitude, we identify the first mode (8.7 GHz for $a = 200$ nm) to be a fundamental mode (mode without any nodal plane) and next modes are higher harmonics with increasing number of nodal planes. In this case, the decrease of separation between nearest antidots results in an increase of the wavenumbers of the modes confined between antidots and is followed by the increase in their frequencies.

The monotonous change in SW's frequencies with changes in a does not agree with the TR-MOKE results (full dots in Fig. 3(a)). Thus, the observed effect can be related to the impact of the edges of antidots. If some SW excitations are localized at the edges of the antidots, then those modes will contribute in very small amount to the TR-MOKE signal for the samples with large a. The edge effects will increase with decreasing a. To understand this observation, we assume the formation of shell like structures at the edges. These shells are formed by bombardment of the Ga ions onto the ML film during FIB milling and the structural, and magnetic properties within those shells may get significantly modified to the extent that a regular structure of $[Co(0.75\,nm)/Pd(0.9\,nm)]_8$ ML may get destroyed. Therefore, a decrease of the effective magnetization, exchange

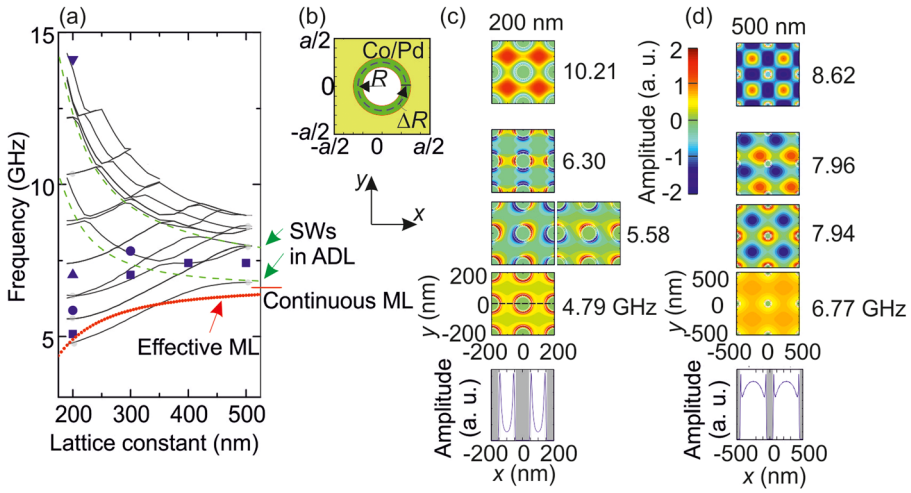

FIG. 3. (a) Dependence of the frequency of SW excitations in ADL with shells (ADLS) on the lattice constant at $\mu_0 H = 0.084$ T. The full blue symbols represent frequencies extracted from the TR-MOKE data (Fig. 2(b)). The frequency of the SW in continuous ML is marked by the red line, the two dashed green lines point at the SW in the ADL without shells. The dotted red line shows the frequency of SW in the film of the effective parameters. (b) The unit cell of the ADL with shell. (c) and (d) Amplitude of the dynamical component of the magnetization vector in ADLS. The profiles of five modes with the lowest frequencies for $a = 200$ nm and 500 nm are shown. At the bottom, the amplitude of the SW excitation with the lowest frequency (the first mode) in ADLS across the center of the unit cell along x axis.

interactions, and especially the PMA field in the shell regions around antidots is expected.[22] One may expect a gradual variation in magnetic properties from the outermost edge to radially inwards of the shell and also a possible reorientation of magnetization due to degradation of PMA. However, PWM does not offer such a possibility for modelling precise changes in the magnetic properties near the edges of the antidots. Instead, we propose a simplified model, which (as we will show later) reproduces the main features of the measured spectra. We consider that an ADL consists of two magnetic materials: one, with the properties of the continuous ML (used above) and the second the material of the shells (of the width ΔR) around the antidots. The unit cell of an antidot lattice with shell (ADLS) structure is shown in Fig. 3(b).

The pinning of SW dynamics at the antidot edges can additionally influence the SW spectra in ADLS; thus, to mimic the various pinning conditions in the theoretical model, we also extended the shell into the hole interior. Such approach is known from the study of SW dynamics in stripes.[16,17] The antidot size is decreased from $R = 50$ nm by putting the circular shell centred at $R = 50$ nm (extended from $R - \Delta R/2$ to $R + \Delta R/2$). As it is very difficult to measure the values of M_S and A characteristic for the shell region of the ADLS, these parameters were used as fitting parameters to obtain an agreement with the TR-MOKE data. We have chosen here shells of width $\Delta R = 17$ nm, $M_S = 0.3 \times 10^6$ A/m, $A = 0.2 \times 10^{-11}$ J/m, and $\mu_0 H_{ani} = 0.03$ T.

The result of calculations for ADLS in dependence on lattice constant is shown in Fig. 3(a) with solid black lines. We can distinguish two families of modes: one with decreasing frequency with increasing a (they follow the dependence found for ADL without the shells) and the second with increasing frequency with increasing a. Based on the analysis of the profiles of SWs shown in Figs. 3(c) and 3(d), we can attribute these two groups of modes to the bulk modes of ADL and modes localized in the shells—we will refer to these SW excitations as shell modes. The first bulk mode (with a quasiuniform distribution of the SW amplitude between the antidots) is located at 10.21 GHz. With the increase in a, the frequency of the fundamental mode decreases, and, at some values of a, it crosses or anti-crosses with the family of shell modes. For $a = 500$ nm, the first mode (at 6.77 GHz) is a fundamental mode, however, still with visible contribution from the shell mode—similar as the second mode. The other modes shown in Fig. 3(d) are bulk modes with nodal planes (e.g., mode at 7.96 GHz) or bulk modes mixed with shell modes (e.g., modes at 7.94 and 8.62 GHz). At $a = 400$ nm, the first mode is at 6.47 GHz, while at $a = 200$ nm, its frequency drops to 4.79 GHz, i.e., both below SW frequency of the continuous ML. The interesting question is why the frequency of shell modes decreases with decreasing a, even below the frequency of the continuous ML (6.63 GHz, marked with the horizontal red bar in Fig. 3(a))? As there is no change in the material parameters with a, we believe that one of the reasons for this behaviour is the impact of collective dynamics of shell modes.

The decrease of the SW frequency with decreasing lattice constant was already reported[12] for the SW mode in the ADL based on Py thin film with in-plane magnetization. This mode was found to be the edge mode. The decrease of the frequency and the increase of its group velocity were attributed to the local decrease of the internal magnetic field and tunnelling mediated coupling between modes in neighbouring areas of localization. We can also attribute the dependence found in our measurement and calculations to the increase of interactions between the shell modes. However, in our case, the static demagnetizing field does not play a significant role. Thus, we can conclude that at a small lattice constant, ($a < 300$ nm) in the ADLS, the dynamic coupling between the SW shell modes is efficient to decrease the coupled mode frequency below the frequency of the continuous ML.

In Fig. 3(a), we have also plotted (red dotted line) the ferromagnetic resonance frequency of the effective ML film

with the M_S and H_{ani} being weighted average of the ML and the material of the shell in dependence on a. This dependence describes the decrease of the uniform mode frequency with decrease in a but does not explain the localization of the SW amplitude and broad band of modes found in the TR-MOKE measurements (Fig. 1(c)).

The coupling between the shell modes may be due to the dynamic dipolar coupling. In fact, the decrease of frequency of SW modes with decreasing lattice constant was observed for the fundamental mode in a chain of ferromagnetic dots (or in an array of ferromagnetic stripes) when the magnetic field was perpendicular to the axis of the chain (or along the stripe).[23–25] However, in our study, the distance between peaks of the shell modes even for $a = 200$ nm (which is $\sim$100 nm) significantly exceeds the ML thickness, thus the dipole coupling is expected to be weak. Moreover, a similar decrease of higher order shell mode frequencies (i.e., modes with the phase changes around the shells—in Fig. 3(c), these are two modes at 5.58 GHz and one at 6.30 GHz) with decreasing a is also found in calculations. These properties indicate that the dipolar coupling may not play an important role here.

At the bottom of Fig. 3(c) and 3(d), we plotted the amplitudes of the first mode along the x-axis crossing the centre of antidots [i.e., along the line marked on the profile of the first mode in Fig. 3(c)] for ADLS with lattice constant $a = 200$ and 500 nm. For $a = 200$ nm, we can see that the amplitude is dominated by SWs localized in the shells, while for 500 nm, a broad fundamental mode (bulk mode) is observed in between antidots still with some contributions from the shell modes. Note that the SW amplitude between the neighbouring shells (in the bulk of ADLS) is different from zero. Therefore, we can expect to have a coupling, due to the overlap of SWs amplitudes localized in neighbouring shells for all considered lattice constants. The presence of magnetic material between shells can additionally provide capability for dynamical exchange coupling between SW excitations. But the elucidation of the role of various possible couplings between the shell modes in ADLS with PMA needs further experimental and theoretical investigations.

The bias field dependence of the SW modes for $a = 200$ nm was also reproduced reasonably well by the calculations as shown in Fig. 2(b), and confirmed the proposed model. The deviations at lower field values (<0.04 T) can be attributed to the reorientation of magnetization at the edges of the antidots due to a degraded PMA which results in mode softening and non-linear dependences of frequencies on the bias field which is impossible to incorporate in the PWM calculations rigorously.

In summary, we have investigated the collective SW dynamics in ADLs in thin $[Co(0.75\,nm)/Pd(0.9\,nm)]_8$ ML with PMA. With TR-MOKE microscopy, we have measured the SW excitations in a series of ADLs with different lattice constants and with fixed antidot radius. We have found a decrease of the frequency of SW with increasing density of antidots, down to values well below the FMR frequency of the continuous ML. Based on the PWM calculations, we have found that these excitations are connected with the SW modes localized in the shells around the antidots. The shells were created during fabrication of the antidots by Ga ion bombardment, and are characterized by modified magnetic properties as compared to the bulk areas of magnetic material in ADL. Moreover, we have shown that this decrease of SW frequencies is driven by a dynamical coupling between the localized modes within the shells. Even though the exact nature of the coupling is debatable, we propose that tunnelling and exchange interactions play important roles. We have demonstrated that in ADL based upon magnetic MLs with PMA, localized and collective SW excitations are possible. This different collective behaviour is important for exploiting the magnonic field of research and to explore the properties of perpendicular percolated media for various technological applications.

We acknowledge the financial assistance from Department of Science and Technology Government of India under Grant No. SR/NM/NS-09/2011, S. N. Bose National Centre for Basic Sciences for Project No. SNB/AB/12-13/96, and NCN of Poland project DEC-2012/07/E/ST3/00538. S.P. acknowledges University Grants Commission for a senior research fellowship. The calculations presented in this paper were performed at the Poznan Supercomputing and Networking Center.

[1]D. Tripathy and A. O. Adeyeye, New J. Phys. **13**, 023035 (2011).
[2]S. Pal, B. Rana, O. Hellwig, T. Thomson, and A. Barman, Appl. Phys. Lett. **98**, 082501 (2011).
[3]S. Pal, B. Rana, S. Saha, R. Mandal, O. Hellwig, J. Romero-Vivas, S. Mamica, J. W. Klos, M. Mruczkiewicz, M. L. Sokolovskyy, M. Krawczyk, and A. Barman, J. Appl. Phys. **111**, 07C507 (2012).
[4]S. N. Piramanayagam, M. Ranjbar, H. K. Tan, W. C. Allen Poh, R. Sbiaa, and T. C. Chong, J. Appl. Phys. **111**, 07B916 (2012).
[5]M. T. Rahman, N. N. Shams, C. H. Lai, J. Fidler, and D. Suess, Phys. Rev. B **81**, 014418 (2010).
[6]V. Neu, C. Schulze, M. Faustini, J. Lee, D. Makarov, D. Suess, S.-K. Kim, D. Grosso, L. Schultz, and M. Albrecht, Nanotechnology **24**, 145702 (2013).
[7]B. Lenk, H. Ulrichs, F. Garbs, and M. Münzenberg, Phys. Rep. **507**, 107 (2011).
[8]V. V. Kruglyak, S. O. Demokritov, and D. Grundler, J. Phys. D: Appl. Phys. **43**, 264001 (2010).
[9]M. Kostylev, G. Gubbiotti, G. Carlotti, G. Socino, S. Tacchi, C. Wang, N. Singh, A. O. Adeyeye, and R. L. Stamps, J. Appl. Phys. **103**, 07C507 (2008).
[10]H. Ulrichs, B. Lenk, and M. Münzenberg, Appl. Phys. Lett. **97**, 092506 (2010).
[11]S. Neusser, B. Botters, and D. Grundler, Phys. Rev. B **78**, 054406 (2008).
[12]S. Neusser, G. Duerr, S. Tacchi, M. Madami, M. L. Sokolovskyy, G. Gubbiotti, M. Krawczyk, and D. Grundler, Phys. Rev. B **84**, 094454 (2011).
[13]R. Zivieri, S. Tacchi, F. Montoncello, L. Giovannini, F. Nizzoli, M. Madami, G. Gubbiotti, G. Carlotti, S. Neusser, G. Duerr, and D. Grundler, Phys. Rev. B **85**, 012403 (2012).
[14]R. Mandal, P. Laha, K. Das, S. Saha, S. Barman, A. K. Raychaudhuri, and A. Barman, Appl. Phys. Lett. **103**, 262410 (2013).
[15]O. Hellwig, T. Hauet, T. Thomson, E. Dobisz, J. D. Risner-Jamtgaard, D. Yaney, B. D. Terris, and E. E. Fullerton, Appl. Phys. Lett. **95**, 232505 (2009).
[16]B. Rana and A. Barman, SPIN **3**, 1330001 (2013).
[17]D. Kumar, J. W. Kłos, M. Krawczyk, and A. Barman, J. Appl. Phys. **115**, 043917 (2014).
[18]S. Tacchi, G. Duerr, J. W. Klos, M. Madami, S. Neusser, G. Gubbiotti, G. Carlotti, M. Krawczyk, and D. Grundler, Phys. Rev. Lett. **109**, 137202 (2012).
[19]M. Krawczyk, S. Mamica, M. Mruczkiewicz, J. W. Klos, S. Tacchi, M. Madami, G. Gubbiotti, G. Duerr, and D. Grundler, J. Phys. D: Appl. Phys. **46**, 495003 (2013).

[20]S. Mamica, M. Krawczyk, M. L. Sokolovskyy, and J. Romero-Vivas, Phys. Rev. B **86**, 144402 (2012).
[21]R. S. Iskhakov, N. A. Shepeta, S. V. Stolyar, L. A. Chekanova, and V. Y. Yakovchuk, JETP Lett. **83**, 28 (2006).
[22]J. M. Shaw, S. E. Russek, T. Thomson, M. J. Donahue, B. D. Terris, O. Hellwig, E. Dobisz, and M. L. Schneider, Phys. Rev. B **78**, 024414 (2008).
[23]P. S. Keatley, P. Gangmei, M. Dvornik, R. J. Hicken, J. Grollier, and C. Ulysse, Phys. Rev. Lett. **110**, 187202 (2013).
[24]B. Pigeau, C. Hahn, G. de Loubens, V. V. Naletov, O. Klein, K. Mitsuzuka, D. Lacour, M. Hehn, S. Andrieu, and F. Montaigne, Phys. Rev. Lett. **109**, 247602 (2012).
[25]M. P. Kostylev, A. A. Stashkevich, and N. A. Sergeeva, Phys. Rev. B **69**, 064408 (2004).